Copper nanoparticle cues for biomimetic cellular assembly of crosslinked elastin fibers

Chandrasekhar R. Kothapalli[a] and **Anand Ramamurthi**[a,b,*]

a *Clemson University-Medical University of South Carolina Bioengineering Program, Charleston, SC 29425, USA*

b *Department of Cell Biology and Anatomy, Medical University of South Carolina, Charleston, SC 29425, USA*

Abstract

Elastin, a structural protein distributed in the extracellular matrix of vascular tissues, is critical to maintaining the elastic stability and mechanical properties of blood vessels, as well as regulating cell-signaling pathways involved in vascular injury response and morphogenesis. Pathological degradation of vascular elastin or its malformation within native vessels and the poor ability to tissue engineer elastin-rich vascular replacements due to innately poor elastin synthesis by adult vascular cells can compromise vascular homeostasis, and must thus be addressed. Our recent studies attest to the utility of hyaluronan (HA) oligomers for elastin synthesis and organization by adult vascular smooth muscle cells (SMCs), though the elastin matrix yields in these cases were quite low relative to total elastin produced. Thus, in this study, we investigated the utility of copper (Cu^{2+}) ions to enhance cellular elastin deposition, crosslinking and maturation into structural fibers. Copper nanoparticles (CuNPs; 80–100 nm) in the dose range of 1–100 ng ml^{-1} were tested for Cu^{2+} ion release, and based on mathematical modeling of their release profiles, CuNPs (1, 10 and 400 ng ml^{-1}) were chosen for supplementation to adult SMC cultures. The 400 ng ml^{-1} dose of CuNPs cumulatively delivered Cu^{2+} doses in the range of 0.1 M, over the 21 day culture period. It was observed that while exogenous CuNP supplements do not upregulate tropoelastin production by vascular SMCs, they promoted formation of crosslinked elastin matrices. The deposition of crosslinked matrix elastin was further improved by the additional presence of HA oligomers in these cultures. Immunofluorescence imaging and structural analysis of the isolated elastin matrices indicate that amorphous elastin clumps were formed within non-additive control cultures, while aggregating elastin fibrils were observed within SMC cultures treated with CuNPs (1–10 ng ml^{-1}) alone or together with HA oligomers. The presence of 400 ng ml^{-1} of CuNPs concurrent with HA oligomers furthered aggregation of these elastin fibrils into mature fibers with diameters ranging from 200 to 500 nm. Ultrastructural analysis of elastin matrix within cultures treated with HA oligomers and 400 ng ml^{-1} of CuNPs suggest that elastin matrix deposition as stimulated by Cu^{2+} ions proceeds via a fibrillin-mediated assembly process, with enhanced crosslinking occurring via stimulation of lysyl oxidase. Overall, the data suggest that CuNPs and HA oligomers are highly useful for regenerating crosslinked, fibrillar elastin matrices by adult vascular SMCs. These results have immense utility in tissue engineering vascular replacements.

*Corresponding author. 173 Ashley Avenue, BSB 601, Medical University of South Carolina, Charleston, SC 29425, USA. Tel.: 001-843-792-5853; fax: 001-843-792-0664; e-mail: aramamu@clemson.edu.

1. Introduction

Elastic fibers, composed of amorphous elastin and associated microfibrillar proteins (e.g. fibrillin), are primarily responsible for the extensibility and resilience of connective tissues such as lungs, skin and blood vessels [1]. Elastic fibers and their components are also involved in signaling vascular cells via their surface receptors, to modulate their proliferation and phenotype [2,3]. Thus, the failure to reinstate a healthy elastin matrix, when these fibers are damaged by injury or disease, or when they are congenitally malformed or absent, can severely compromise vessel homeostasis [4]. In this context, active regeneration of elastin matrices in vivo and within tissue-engineered constructs provides an alternative promising approach [5].

Current tissue engineering strategies for elastin regeneration in situ are limited by very poor tropoelastin mRNA expression by adult vascular cells and the unavailability of scaffolds that can provide biomolecular cues necessary for cellular-mediated regeneration of native elastin mimics [6]. Although synthetic elastomers or elastin peptide assemblies can replicate the mechanics of native elastin [7,8], the absence of cell-signaling microfibrillar proteins (e.g. fibrillin) prevents the construct from eliciting native responses from vascular SMCs [9]. Based on earlier studies which suggested close association between several glycosaminoglycan (GAG) types (e.g. hyaluronic acid) and elastin within vascular tissues [10,11], we recently showed that the elastogenic effects of hyaluronan (HA) are highly fragment-specific, with HA fragments (<1 MDa) and shorter oligomers (<1 kDa) being more cell-interactive and elastogenic than the relatively bioinert long-chain HA (>1 MDa) [12–15]. We determined that HA oligomers, specifically, stimulate multifold increases in the production of soluble tropoelastin and crosslinked matrix elastin, and enhance elastin fiber assembly and the synthesis of lysyl oxidase (LOX, an elastin and collagen crosslinking enzyme) and desmosine crosslinks [13]. In follow-up studies, we showed that these "elastogenic" effects could be synergistically enhanced by stimulating cells with HA oligomers together with other growth factors (e.g. TGF-β1, IGF-1) [14,15]. These studies attested to the tremendous potential of HA oligomers, alone, or together with other growth factor cues, with respect to elastin matrix regeneration.

Although our studies demonstrated the utility of HA oligomers for increasing tropoelastin and total elastin (matrix elastin + tropoelastin) production on a per-cell basis, the net amount of crosslinked matrix elastin relative to the total elastin produced, defined as elastin matrix yield, remained low (~10–20%) [12–14]. This emphasizes the need to provide other exogenous "elastin maturation cues" to enhance cellular LOX production or LOX enzyme activity, to enhance elastin crosslinking or render it more efficient [16,17]. Since extracellular LOX availability and activity are dependent on the presence of copper ions (Cu^{2+}) [18], we hypothesize that the simultaneous delivery of HA oligomers and Cu^{2+} cues will enhance tropoelastin recruitment and crosslinking into mature elastin matrix. Thus, the objective of the current study is to evaluate the benefits of Cu^{2+} ion delivery concurrent with elastogenic cues (i.e. HA oligomers) on elastin crosslinking in a culture model of adult rat aortic smooth muscle cells (RASMCs). Since sudden exposure of vascular cells to Cu^{2+} ions provided at high doses, via exogenous supplementation of soluble copper salts, appears to induce some cytotoxicity and cell death [19–21], we now seek to determine if gradual release of Cu^{2+} ions from copper nanoparticles (CuNPs) concurrent with HA oligomeric cues can improve recruitment and crosslinking of soluble tropoelastin precursors, and facilitate their assembly into mature fibers. If shown to be beneficial, CuNP cues for elastin maturation will in the future be delivered

together with other elastogenic cues (e.g. HA oligomers and growth factors) to simultaneously enhance elastin precursor and matrix synthesis, and maximize the yield of matrix elastin within tissue-engineered constructs.

2. Materials and methods

2.1 Copper ion release from CuNPs

To estimate the amounts of CuNPs (80–100 nm; Sigma-Aldrich, St Louis, MO) necessary to generate Cu^{2+} ion concentrations of the order of 0.1 M, which in an earlier study [22] were shown to significantly enhance elastin crosslinking, but to be mildly cytotoxic, we fitted the Cu^{2+} ion release profiles experimentally generated with three randomly selected concentrations of (1, 10, 100 ng ml^{-1}) of CuNPs, to a mathematical model. We quantifed the concentration of Cu^{2+} ions in solution using an atomic absorption spectroscope (PerkinElmer Model 3030, PerkinElmer, Norwalk, CT), fitted with a copper lamp. Briefly, the nanoparticles were dispersed in 5 ml of distilled water (pH 7) at each of the above concentrations. The Cu^{2+} ion content in 1 ml aliquots of these solutions was measured at regular intervals over a 30 day period, and cumulative Cu^{2+} release calculated. The spent aliquots were replaced with 1 ml fresh distilled water, and the concentration of Cu^{2+} ions in the removed aliquots was accounted for in calculating the cumulative release of Cu^{2+} ions. All measurements were done in triplicate and the Cu^{2+} ion concentrations expressed in moles.

The experimental Cu^{2+} release profiles were then fit to a mathematical model, and that model was used to predict a CuNP dose that would cumulatively release approximately 0.1 M of Cu^{2+} ions over the 21 day period of culture. This process eliminated the innumerable "trial-and-error" experiments that would otherwise have been necessary to identify an "effective" CuNP dose. The dependence of Cu^{2+} ion release on CuNP concentration and time was fit using a hierarchical regression analysis, wherein a new predictor is added to or dropped from those used in the previous analysis based on the statistical significance of a particular model. The quadratic regression model which can accommodate linear, curvature and interdependence of the time (x) and CuNP concentration (y) used in this study was:

$$R = a + b*x + c*y + d*x*y + e*x^2 + f*y^2, \tag{1}$$

where R represents the amount of Cu^{2+} ions released, and a-f are the estimated regression coefficients. After initialization with the full quadratic regression model given in Eq. (1), a backward elimination procedure was used to reduce the number of terms in the model until all the remaining terms were statistically significant ($P < 0.05$). Based on this modeling, it was estimated that 400 ng ml^{-1} of CuNPs would cumulatively release ~0.1 M of Cu^{2+} ions over the 21 day culture period, assuming no fouling occurs within the media.

2.2 Cell culture

HA oligomer mixtures, which were provided to cells as elastogenic cues, contained predominantly 4-mers (75 ± 15% w/w, with 6-mers and 8-mers forming the balance). These mixtures were prepared in our lab using protocols we have previously reported [13]. Briefly, 20 mg of HMW HA (Genzyme Biosurgery, Cambridge, MA) was enzymatically digested with bovine testicular hyaluronidase (3.6 mg, 451 U mg^{-1}; Sigma-Aldrich, St Louis, MO) in 4 ml of digest buffer (150 mM NaCl, 100 mM CH_3COONa, 1 mM Na_2EDTA, pH 5.0) for 18 h at 37°C. The enzyme activity was terminated by boiling the mixture in a waterbath for 5 min following digestion; the mixture was then dialyzed against water for 12 h, and frozen until use at −20°C.

Low passage (3–5) RASMCs (Cell Applications, San Diego, CA) were selected for the current study due to their relatively lower levels of tropoelastin production compared to neonatal cells, thus rendering them of greater relevance to regeneration of elastin-rich constructs from adult cells. RASMCs were seeded onto 6-well tissue culture plates (BD Labware, Bedford, MA) at a density of 3×10^4 cells well^{-1} and cultured with DMEM-F12 (Invitrogen, Carlsbad, CA) containing 10% v/v fetal bovine serum and 1% v/v Penstrep (VWR Scientific, West Chester, PA). HA oligomers prepared in serum-rich medium were added to cell cultures at an ultimate dose of 0.2 μg ml^{-1}. CuNPs dispersed in distilled water were supplemented exogenously to the culture wells at final doses of either 1, 10 or 400 ng ml^{-1}, except in control cultures which received no supplements. The culture medium was replaced twice weekly, and the spent medium from each well was pooled over the 21 day culture period and frozen for further biochemical analysis.

2.3 DNA assay for cell proliferation

The DNA content of cell layers was estimated using a fluorometric method described by Labarca and Paigen [23]. Briefly, cell layers at 1 and 21 days of culture were detached with 0.25% v/v trypsin–EDTA, pelleted by centrifugation, resuspended in 1 ml of NaCl/Pi buffer (4 M NaCl, 50 mM Na$_2$HPO$_4$, 2 mM EDTA, 0.02% sodium azide, pH 7.4), and a 100 μl aliquot assayed. The DNA in the sonicated aliquot was measured using the fluorometric assay and the cell count was used to normalize the measured amounts of synthesized matrix for reliable comparison between experimental cases.

2.4 Hydroxyproline (OH-Pro) assay for collagen

Collagen incorporated within cell layers cultured over 21 days, and collagen released by the cells into the pooled medium over the same period were quantified using a hydroxyl-proline assay, as described previously [24]. Briefly, the cell layers were homogenized in distilled water, pelleted by centrifugation (10000g, 10 min) and digested with 1 m; of 0.1 N NaOH (1 h, 98° C). The digestate was centrifuged to isolate a mass of insoluble, crosslinked elastin. The supernatant containing solubilized collagen and immature matrix elastin was neutralized with an equal volume of 12 N HCl, and divided into two equal volumetric halves; one half-volume was hydrolyzed at 110°C for 16 h, and dried in a constant stream of N$_2$ gas overnight and 20 μl aliquots of the reconstituted residue were assayed for OH-Pro content. The amounts of matrix-derived collagen (i.e. in the cell layers) and soluble collagen (in pooled medium fraction) were calculated on the basis of the 13.2% content of OH-Pro in collagen.

2.5 Fastin assay for elastin

Elastin was quantified using a Fastin assay (Accurate Scientific Corp, Westbury, NY), as described previously [12]. Since the Fastin assay quantifies only soluble α-elastin, the matrix elastin from the cell layer was first rendered to a soluble form. To do this, the harvested cell layers were digested with 0.1 N NaOH (1 h, 98°C) and centrifuged (2000 g, 15 min) to isolate an alkali-insoluble elastin pellet from a supernatant containing alkali-soluble elastin (S1 fraction). The alkali-insoluble elastin pellet, representing highly crosslinked matrix elastin, was dried to a constant weight, solubilized with two cycles of digestion with 0.25 N oxalic acid (1 h/cycle, 95°C), and the pooled digests filtered in microcentrifuge tubes fitted with 10 kDa cut-off membranes to obtain soluble α-elastin (S2 fraction). The number of cycles of digestion with oxalic acid was optimized so as to render the insoluble matrix elastin into a soluble form, fit for quantification with the Fastin assay. Finally, the digestates S1 and S2 were neutralized with equal volumes of 12 N HCl, hydrolyzed (110°C, 16 h), dried in a constant stream of N$_2$ gas overnight and reconstituted in 20 μl of deionized (DI) water for direct elastin protein quantification using the dye-binding Fastin assay. Separately, spent fractions of culture medium pooled for each well at biweekly intervals over the 3 week culture period were also

lyophilized, reconstituted in DI water, and then directly assayed for tropoelastin using the Fastin kit. Thus total elastin amount was measured as the sum of the alkali-soluble matrix elastin (from S1 fraction), alkali-insoluble (crosslinked) matrix elastin (from S2 fraction) and elastin precursors (tropoelastin) in the pooled spent media. The volume-corrected amounts of synthesized matrix were normalized to the respective DNA amounts to provide a reliable basis of comparison between samples, and to broadly assess if the observed changes in the amount of matrix synthesized could possibly be due to increases in elastin production on a per cell basis.

2.6 Western blot analysis for (LOX synthesis

Western blot analysis was performed using methods described previously [12] to semi-quantitatively assess the benefits, if any, of LOX protein synthesis. Briefly, aliquots of spent medium from cultures were pooled at biweekly intervals over the 21-day culture period, lyophilized, assayed for protein content using a DC protein assay kit (Biorad Corporation, Hercules, CA) to further optimize sample volumes for SDS PAGE/Western blot. Protein bands were detected with primary rabbit $\times$ rat polyclonal antibodies to the 31 kDa active LOX protein (Santa Cruz Biotechnology, Santa Cruz, CA), visualized and quantified using a Chemi-Imager IS 4400 system (Alpha Innotech, San Leandro, CA).

2.7 LOXfunctional activity

Spent culture medium pooled at day 21 of RASMC culture was assayed for LOX enzyme activity using a fluorometric assay based on generation of H_2O_2 when LOX acts on a synthetic substrate. H_2O_2 was detected using an Amplex red kit (Molecular Probes, Eugene, OR) as described previously [25]. The fluorescence intensities were recorded with excitation and emission wavelengths at 560 and 590 nm, respectively. Although the assay might also detect semicarbazide-sensitive amine oxidase (also known as Vascular Adhesion Protein-1 or VAP-1), this is not expected to interfere with the assay in this study, since cultured smooth muscle cells do not express VAP-1 [26].

2.8 Assay for desmosine crosslinks

Desmosine crosslink densities within elastin matrices were quantified using ELISA to determine if any of the provided cues enhanced efficiency of elastin crosslinking [12]. At 21 days of culture, cell layers were digested with collagenase (12 h, 37°C) and elastase (12 h, 37°C), the digestates acid-hydrolyzed (6 N HCl, 110°C, 16 h), and the desmosine content in the reconstituted dried residues determined by ELISA, and compared to corresponding trends in insoluble matrix elastin.

2.9 Immunoflourescence detection of elastin, fibrillin and LOX

Immunofluorescence techniques were used to confirm elastin, fibrillin and LOX expression by cells that were cultured under conditions deemed through biochemical analyses to be important to up-regulate elastin synthesis. RASMCs were seeded in 4-well sterile chamber slides at 5×10^3 cells/well and cultured with HA oligomers and CuNPs as described in Sec. 2.2. At 21 days, the cell layers were fixed with 4% w/v paraformaldehyde for 10 min, and labeled with Alexa 488 Phalloidin (Molecular Probes, Eugene, OR; 1:20 dilution; 20 min, 25°C), a marker for smooth muscle cell F-actin. The target proteins were detected with rabbit polyclonal antibodies to elastin, fibrillin-1 (Elastin Products Company, Owensville, MO), and LOX (Santa Cruz Biotechnology), and visualized with a Rhodamine-conjugated donkey anti-rabbit IgG secondary antibody (Abcam, Cambridge, MA) on a fluorescence microscope. Cell nuclei were visualized with the nuclear stain 4′, 6-diamino-2--phenylindole dihydrochloride (DAPI) contained in the mounting medium (Vectashield; Vector Labs, Burlingame, CA).

2.10 Elastin matrix ultrastructure

Scanning electron microscopy was used to discern the structural organization of matrix elastin within cell layers cultured with or without exogenous HA oligomers and the provided doses of Cu^{2+} ions. For sample preparation, medium-aspirated cell layers were incubated in 1 N NaOH for 2 h at 60°C to digest cellular material and non-elastin matrix components, rinsed in PBS, fixed with 2% w/v glutaraldehyde (4°C, 1 h) and treated with increasing ethanol gradient series (60–100% v/v, each for 15 min). The dried matrix layers were sputter gold-coated at 30 mA for 1 min, and visualized in a Hitachi S4800 field emission scanning electron microscope.

Transmission electron microscopy was used to characterize the ultrastructure of the elastin matrix in select cultures (treated with 400 ng ml^{-1} of CuNPs and HA oligomers). Control and test cell layers were fixed with 2.5% v/v glutaraldehyde, postfixed in 1% v/v osmium tetroxide (1 h), dehydrated in graded ethanol, embedded in Epon 812 resin, sectioned, placed on copper grids, stained with uranyl acetate and lead citrate, and visualized on a Hitachi H7600 transmission electron microscope [12].

2.11 Statistical analysis

All experiments were performed in triplicate and quantitative results reported as means ± SD. Statistical significance between and within groups was determined using two-way ANOVA. Results are deemed significantly different from controls for $P < 0.05$.

3. Results

3.1 Copper ion release from CuNPs

Fig. 1 shows the release profiles of Cu^{2+} ions for three different CuNP doses. While there were no significant differences in the release profiles of Cu^{2+} ions between 1 and 10 ng ml^{-1} of CuNPs, 100 ng ml^{-1} of CuNPs generated significantly more Cu^{2+} ions. It was observed that over the 30 day period, 1 and 10 ng ml^{-1} of CuNPs resulted in cumulative release of ~0.03 M of Cu^{2+} ions, while 100 ng ml^{-1} CuNPs resulted in cumulative release of ~0.05 M of Cu^{2+} ions. As seen from the modeling curves shown in Fig. 1, the predictions fit quite closely the experimentally measured values ($P = 0.001$ for all the parameters and the overall fit; number of degrees of freedom for each fit = 29). Based on this mathematical analysis, we predict that a CuNP dose of 400 ng ml^{-1} would be required to generate Cu^{2+} ion release equivalent to 0.1 M over a 21 day period. The predicted Cu^{2+} ion release profile from 400 ng ml^{-1} of CuNPs is also shown in Fig. 1.

3.2 Cell proliferation

In Fig. 2A, proliferation ratios (ratio of cell number at day 21 to cell number at day 1) of RASMCs cultured in the presence of either CuNPs alone (black bars) or together with HA oligomers (white bars) are shown normalized to proliferation ratios determined for control cultures. At 3 weeks, proliferation ratios within cell layers cultured with 1, 10 and 400 ng ml^{-1} of CuNPs were 1.54 ± 0.15-, 1.84 ± 0.23- and 1.32 ± 0.16-fold of that in non-additive controls, respectively ($P = 0.002$, 0.001 and 0.031 vs. controls). In cultures that received HA oligomers as well, the ratios were also higher than controls (1.35 ± 0.3-, 1.28 ± 0.3- and 0.92 ± 0.2-fold, respectively vs. controls; $P > 0.2$, in all the cases). Also, differences in cell proliferation ratios between cultures that received both HA oligomers and CuNPs and those that received corresponding doses of CuNPs alone were not statistically significant.

3.3 Elastin protein synthesis

Fig. 2 shows mean ± SD of elastin protein synthesized (n = 3 per case) in the different test cultures, normalized first to their respective cellular DNA contents at 21 days, and further

normalized to the corresponding elastin protein content in non-additive control cultures. Tropoelastin synthesis in cultures that received CuNPs alone or together with HA oligomers was identical to that measured in non-additive controls (28284 ± 5088 ng/ng DNA; $P > 0.2$ in all the cases). Likewise, addition of CuNPs alone or together with HA oligomers had no stimulatory effect on the collagen synthesis (soluble and matrix forms), compared to control cultures (826 ± 125 ng/ng DNA; $P > 0.4$ in all the cases).

Elastin incorporated into the matrix was measured as the sum of two individual fractions, i.e. a highly cross-linked, alkali-insoluble elastin pellet, and an alkali-soluble fraction. As shown in Fig. 2B, of all the tested CuNP doses, only addition of 400 ng ml^{-1} of CuNPs increased synthesis of alkali-soluble elastin by 1.54 ± 0.08-fold; concurrent supplementation of HA oligomers to these cultures furthered this increase to 2.16 ± 0.26-fold, relative to non-additive controls (6931 ± 1200 ng/ng DNA; $P < 0.001$ vs. controls, in both the cases). Lower concentrations of CuNPs (1 and 10 ng ml^{-1}) alone or together with HA oligomers, on the other hand, suppressed alkali-soluble matrix elastin production relative to non-additive controls ($P < 0.01$ in all cases vs. controls).

While culture with 1 ng ml^{-1} supplements of CuNPs alone caused a $38 \pm 4\%$ decrease in the production of alkali-insoluble (crosslinked) matrix elastin relative to control cultures (183 ± 29 ng/ng DNA), concurrent delivery of HA oligomers enhanced the same by 2.7 ± 0.18-fold over control levels ($P < 0.001$ vs. controls; Fig. 2C). When 10 and 400 ng ml^{-1} of CuNPs were supplemented, alone or concurrently with HA oligomers, crosslinked elastin production increased by 1.26 ± 0.6- and 1.24 ± 0.09-fold, respectively ($P = 0.8$ and 0.001 vs. controls), and by 1.99 ± 0.18- and 3.14 ± 0.03-fold ($P < 0.001$ vs. controls), respectively. The trends in total matrix elastin synthesis by RASMCs (Fig. 2D) reflected those observed in alkali-soluble matrix elastin synthesis (Fig. 2B). When 400 ng ml^{-1} of CuNPs was added, alone or together with HA oligomers, total matrix elastin synthesis increased by 1.6 ± 0.1- and 2.28 ± 0.23-fold ($P < 0.001$ vs. controls in both cases), respectively. Lower concentrations of CuNPs (1 and 10 ng ml^{-1}), alone or together with HA oligomers, suppressed alkali-soluble matrix elastin production ($P < 0.01$ in all cases vs. controls). No significant increase in desmosine crosslink density was measured in test cultures compared to non-additive control cultures (0.92 ± 0.05-, 0.65 ± 0.21- and 0.64 ± 0.1-fold in 1, 10 and 400 ng ml^{-1} of CuNP-alone cultures, respectively; 0.91 ± 0.23-, 0.9 ± 0.05- and 0.94 ± 0.2-fold in CuNP- and HA oligomer-supplemented cultures, respectively).

Fig. 3A shows the elastin matrix yields (yield = matrix elastin/(tropoelastin + matrix elastin)) calculated from the elastin amounts shown in Fig, 2. While only $20.1 \pm 3.5\%$ of total elastin produced in non-additive control cultures was incorporated into the matrix, the elastin matrix yield was $61.3 \pm 3.6\%$ in those cultured with 400 ng ml^{-1} of CuNPs alone, and $58.8 \pm 6.1\%$ in those that received HA oligomers as well. Except for matrix elastin yield ($35.5 \pm 3.4\%$) in cultures that received 1 ng ml^{-1} of CuNPs and HA oligomers (Fig. 3A), the yield in the other test cultures was not significantly different than in control cultures.

3.4 LOX protein synthesis and activity

Spent medium fractions pooled over 21 days from test and control cultures were analyzed by Western blot, and the DNA-normalized intensities of the LOX-protein bands within test cultures further normalized to those in controls. Exogenous CuNPs (1, 10, 400 ng ml^{-1}) either alone or together with HA oligomers (1 and 10 ng ml^{-1} only) did not enhance LOX protein synthesis relative to controls (Fig. 3B). LOX protein synthesis was, however, enhanced by 1.67 ± 0.13-fold in the presence of both 400 ng ml^{-1} CuNPs and HA oligomers ($P < 0.01$ vs. controls).

Fig. 3C describes the effect of addition of CuNPs, alone or together with HA oligomers, on LOX enzyme activity. Relative to controls, 1 ng ml^{-1} of CuNPs alone or together with HA oligomers increased LOX activity by 1.09 ± 0.02- and 1.15 ± 0.02-fold, respectively ($P < 0.01$ in both the cases), while the corresponding values obtained with 10 ng ml^{-1} of CuNPs alone were 1.1 ± 0.02- and 1.16 ± 0.01-fold, respectively ($P < 0.01$ in both cases). However, surprisingly, no significant increases in LOX activity were detected on addition of 400 ng ml^{-1} of CuNPs alone, or together with HA oligomers ($P > 0.8$ in both cases vs. controls). It should, however, be noted that the LOX protein expression and activity were measured in the spent cell culture medium and not in the respective cell layers, which might explain the absence of a strong correlation between the increase in crosslinked elastin protein production and the LOX expression/activity within these cultures.

3.5 Immunodetection of elastin, fibrillin and LOX in cell layers

Immunofluorescence micrographs confirmed the presence of elastin, fibrillin and LOX (red fluorescence) both in 21 day cultures that received 400 ng ml^{-1} of CuNPs alone and the same dose of CuNPs together with HA oligomers (Fig. 4). The fluorescence intensity due to elastin was visibly greater in cultures supplemented with CuNPs than in control cultures, and even more so within cultures that also received HA oligomers. Elastin fiber networks were apparent in the latter cultures, while the elastin appeared as homogenous and amorphous masses in control cultures. Fluorescence intensity due to fibrillin was much greater in CuNP-supplemented cultures than in non-additive controls, and was also as pronounced in cultures that also received HA oligomers, thus confirming the fibrillin-mediated matrix elastin deposition in the presence of these additives. Interestingly, while fluorescence due to LOX was sparse in control cultures, intense coloration (red) due to LOX was observed in CuNP-added cultures, and even more so when HA oligomers were concurrently supplemented. Negative control cultures that were untreated with the respective primary antibodies against the studied proteins showed no coloration.

3.6 Structural analysis of matrix elastin

Fig. 5 shows representative scanning electron micrographs of isolated elastin matrices from 21 day cultures. Compared to the non-additive control cultures where elastin was sparingly deposited as amorphous clumps (panel A), addition of CuNPs alone, and together with HA oligomers, enhanced elastin fiber formation. Relative to the presence of nanoparticles alone (1 ng ml^{-1} in panel B; 10 ng ml^{-1} in panel C) where elongated elastin fibers with diameter ranging from 100 to 300 nm are clearly visible, the concurrent presence of HA oligomers promoted deposition of bundles of aggregating elastin fibrils (1 ng ml^{-1} in panel E; 10 ng ml^{-1} in panel F). When 400 ng ml^{-1} of CuNPs was added alone, elastin fiber formation was likewise favored, with a significantly higher density of elastin bundles observed (panel D). Concurrent presence of HA oligomers promoted dense elastin matrix (panel G) containing a greater number of apparently fully formed fibers (~ 300–500 nm diameter; panel H).

Fig. 6 shows representative transmission electron micrographs of elastin matrices within 21 day cultures. Discrete amorphous elastin clumps with relatively few elastin fibers were present in additive-free control cultures (Fig. 6A). CuNPs (400 ng ml^{-1}) stimulated deposition of numerous aggregating elastin fibrils between the cells (Fig. 6B), more densely distributed than in control cultures. However, when both 400 ng ml^{-1} of CuNPs and HA oligomers were supplemented instead (Fig. 6C,D), mature elastin fiber formation was observed, with the matrix containing numerous fully formed bundles of fibers (100–300 nm diameter), more than that observed in control cultures and those that received CuNPs alone. Fibrillin (immunogold particle-stained), which appeared in transverse sections as darkly stained nodules, was located at the periphery of aggregating elastin fiber bundles, signifying normal elastic fiber assembly under these conditions.

4. Discussion

An outstanding problem in the field of vascular tissue engineering is the inadequacy of conventional tissue engineering methods and materials for manufacturing structurally and functionally faithful vascular elastic matrices on demand. This is because cardiovascular tissues are highly complex in their architecture and structural organization, and the capacity of adult vascular cells for self-repair is less effective than what tissue-engineering principles demand. Although fully developed mature elastic fibers are insoluble and inert to local changes in pH and chemical environment, various proteolytic enzymes secreted by SMCs, such as matrix metalloproteinases (MMPs-2, 9, 12) and elastases can degrade elastin fibers and its components [27–29]. The literature suggests that these degradation products can modulate vascular remodeling via their interaction with SMCs [30], leading to structural and mechanical abnormalities in large arteries [31]. Thus, proper assembly and functioning of elastic fibers is critical for maintaining homeostasis in organs and tissues.

As mentioned above, elastic fibers are complex macromolecular structures which contain amorphous elastin and other non-elastin protein components (e.g. fibrillin, elaunin). They are difficult to repair because their deposition pattern requires the coordinated expression of all of the microfibrillar molecules as well as the cross-linking enzymes critical for elastin, so that the correct temporal sequence is followed [1]. Cell-secreted soluble elastin protein precursors, i.e. tropoelastin monomers [32], are recruited by coacervation onto preformed templates of fibrillin-rich microfibrils [33], and stabilized by LOX-catalyzed formation of desmosine crosslinks [34]. Microfibrils, which appear first in the elastic fiber development and associate themselves close to the cell surface, facilitate tropoelastin cross-linking to form the functional polymer [35]. Hence, approaches to elastin regeneration must be able to mimic the spatiotemporal sequence of these events leading to elastin matrix assembly. However, elastin-producing cells in adult tissues often synthesize elastin that does not polymerize or organize into a functional three-dimensional fiber, leading to loss of tissue homeostasis.

Current tissue engineering approaches to regenerate elastin-rich vascular constructs are limited by progressive destabilization of tropoelastin mRNA expression in adult vascular cells [36, 37] and the unavailability of cellular cues necessary to up-regulate elastin synthesis, maturation and organization [6,38]. Thus, an important aspect of tissue-engineering elastin-rich vascular constructs is the ability to regulate the amount, quality, ultrastructure and hierarchical organization of the synthesized elastin precursors, so as to maximize their crosslinking efficiency and matrix formation. In this context, our recent studies strongly attest to the utility of HA-based biomaterials and biomolecular cues for cellular-mediated elastin matrix regeneration [12–14,39]. A key deduction from these studies is that though HA oligomers (<1 kDa) are more biologically active than long-chain HA (>1 MDa), and dramatically increase elastin synthesis and deposition, the elastin matrix crosslinking efficiency is unchanged relative to control cultures [12,13].

Dahl et al. demonstrated the benefits of increasing medium Cu^{2+} concentration to elastin matrix crosslinking efficiency in an engineered vascular-like tissue [40]. Likewise, in our own previous studies [22], we investigated the effects of soluble copper salts, delivering steady-state doses of 0.01 and 0.1 M of Cu^{2+} ions, to elastin matrix deposition, assembly (i.e. fiber formation) and maturation (i.e. crosslinking) in RASMC cultures. Our results suggested that 0.1 M of $CuSO_4$ (but not 0.01 M) and HA oligomers (or HMW HA) significantly improved elastin matrix synthesis, crosslinking and fiber formation by RASMCs. However, cytotoxicity associated with exposure of vascular cells to Cu^{2+} doses of this order of magnitude [21,22], delivered at steady-state levels from soluble copper salts, suggested that more controlled modes of Cu^{2+} ion delivery, such as from CuNPs, may be necessary to deter the same. Thus, in this study, we have sought to deliver a Cu^{2+} dose in the range of 0.1 M via controlled release from

CuNPs and investigated the impact of such delivery with or without HA oligomers on elastin matrix synthesis, assembly and maturation. Since the kinetics of Cu^{2+} ion release from CuNPs was not known, we experimentally measured Cu^{2+} release from three random concentrations of CuNPs (1, 10, 100 ng ml^{-1}), fitted mathematical models to the release profiles, and used the models to predict the dose of CuNPs that would over 21 days theoretically release an equivalent of 0.1 M of Cu^{2+} ions in a serum-free solution. Via this method, we eliminated the need to laboriously determine the desired CuNP dose via trial-and-error experimentation. Detectable amounts of Cu^{2+} ions (~0.0012 M) were released even from 1 ng ml^{-1} of CuNPs within the first 5 h, which showed that exogenous nanoparticles are effective vehicles for even short-term Cu^{2+} ion delivery. From the release profiles, it can be observed that irrespective of CuNP dose, Cu^{2+} ion release peaked within the first 30 h, after which sustained release of ions was maintained. Thus, in effect, Cu^{2+} release over the 21 day culture period can be deemed steady state. Based on our mathematical model, we estimated that in a solution free of any fouling agents (e.g. proteins), 400 ng ml^{-1} of CuNPs would generate ~0.1 M of Cu^{2+} ions over 21 days; in culture medium containing low amounts of serum supplements, the release might be slightly lower due to mild fouling of the CuNP surfaces, but still within the same order of magnitude. Based on this analysis, we tested the utility of 400 ng ml dose of CuNPs to elastin maturation in smooth muscle cell cultures.

A significant observation was that 400 ng ml^{-1} of CuNPs had no cytotoxic effects on SMCs, and thus no apparent change in morphology over the 21 day culture period. In contrast, our previous studies [22] showed that an equivalent dose of Cu^{2+}, released from soluble copper sulfate salt, induced mild cytotoxicity that was apparent within a day of addition, and caused temporary cell rounding and some cell death. Previously, we also showed that in the presence and absence of HA oligomers, supplementation of 0.01 M of Cu^{2+} ions from copper salts increased cell proliferation (1.5–2-fold relative to controls), while 0.1 M of Cu^{2+} ions suppressed the same (80% of controls) [22]. In this study, in the cases where the CuNPs delivered were far less than 0.1 M of Cu^{2+} ions (i.e. 1 and 10 ng ml^{-1} of CuNP doses), a similar 1.5–2-fold increase in cell proliferation over control cultures was observed. However, when a Cu^{2+} dose of the order of 0.1 M was released from 400 ng ml^{-1} of CuNPs, active promotion rather than suppression of cell proliferation was noted. Thus, our experiments show that controlled release of Cu^{2+} ions from CuNPs deters rapid increase in Cu^{2+} concentration in the initial period after cell seeding, and thus may not have long-term toxic effects. In accordance with our earlier observation that 0.2 μg ml^{-1} of HA oligomers inhibits SMC proliferation [15], in this study also, supplementation of HA oligomers to cultures together with CuNPs suppressed cell proliferation down to levels measured in control cultures. Thus, from a tissue engineering perspective, CuNPs and HA oligomers do not promote cell proliferation, but at the same time do not induce cell death thereby in turning adversely impacting matrix synthesis and accumulation within the constructs.

In this study, exogenous CuNPs had no effect on total elastin production, both in the presence and absence of HA oligomers. In general, lower doses of CuNPs (1–10 ng ml^{-1}), alone or together with HA oligomers, as expected offered no benefit to matrix elastin synthesis, except for a 2.7-fold increase in crosslinked elastin synthesis in the presence of 1 ng ml^{-1} of CuNPs and HA oligomers. The lack of any benefits to elastin synthesis mimicked our prior observations when 0.01 M of $CuSO_4$ was supplemented to RASMC cultures [22]. However, production of matrix elastin (both soluble and crosslinked forms) increased multifold with the addition of 400 ng ml^{-1} of CuNPs, both alone and together with HA oligomers, suggesting the effectiveness of these cues in the recruitment and crosslinking of tropoelastin precursors into matrix structures. Since total cellular elastin production was unaffected by these cues, the net result of doubling in matrix deposition is a much higher matrix yield (400 ng ml^{-1} CuNPs alone: 61.3 ± 3.6%; 400 ng ml^{-1} CuNPs and HA oligomers: 58.8 ± 6.1%; control cultures: 20.1 ± 3.5%).

LOX protein synthesis was unchanged in cultures supplemented with CuNPs only (all doses) and those that received the lower doses (1 and 10 ng ml^{-1}) of CuNPs and HA oligomers together. On the other hand, when 400 ng ml^{-1} of CuNPs was added to cultures together with HA oligomers, a significant increase in LOX protein synthesis was observed. Interestingly, in a prior study, we showed that HA oligomers alone have no effect on LOX protein synthesis, suggesting that observed increases in this case are due to CuNPs (400 ng ml^{-1}) and not the HA oligomers. Collectively, these results suggest that (i) CuNP doses (1 and 10 ng ml^{-1}) that generate far less than 0.1 M of Cu^{2+} ions do not induce LOX protein synthesis; (ii) Cu^{2+} concentrations of the order of 0.1 M generated by 400 ng ml^{-1} of CuNPs can potentially stimulate LOX protein synthesis by cells, provided HA is also present; and (iii) HA oligomers which likely interact and bind to cell surface receptors (e.g. CD44, TLR-4) also likely immobilize Cu^{2+} ions via opposite charge interactions, as others have shown possible [41]. Thus, when both CuNPs and HA oligomers are present, it may certainly be possible that Cu^{2+} ions localize close to the cell layer where they may intimately influence cell behavior, including their induction of LOX production by cells and preferred crosslinking of tropoelastin that coacervates on HA [42], close to the cell surface. However, it is not clear at this stage whether this electrostatic binding complex affects intracellular cell signaling cascade, thereby modulating the transcription of elastin gene itself. Our results also show that all provided doses of CuNPs induced marginal, but statistically significant, increases in LOX enzyme, although these increases were deemed not to depend on CuNP dose. In all cases, addition of HA oligomers induced a small but significant increase in LOX activity. Since we showed in an earlier publication that HA oligomers have no impact on LOX activity, the observed increases here may be solely due to opposite charge interactions of CuNPs with HA oligomers and their resultant localization at the cell layer to somewhat enhance activity of endogenous LOX. Regardless, in view of the limited effects on LOX activity, more efficient recruitment and crosslinking of tropoelastin into a matrix may primarily occur due to a combination of greater available LOX amounts and physical proximity of elastin precursors and LOX at the cell layer, rather than due to increases in LOX activity. Another possibility is that the observed elastogenic effects might also be due to the pro-oxidative potential of Cu^{2+} ions released from 400 ng ml^{-1} of CuNPs. However, investigating this hypothesis is beyond the scope of this study.

Structural analysis (electron microscopy) of matrix elastin qualitatively supported the biochemical measurements within CuNP-stimulated cultures. While the control cultures contained only amorphous elastin deposits, aggregating elastin fibers were seen within cultures treated with CuNPs (all doses), alone and together with HA oligomers, with multiple bundles of fully formed elastin fibers with diameter ranging from 200 to 500 nm. Immunofluorescence images confirmed the amorphous and fibrillar nature of elastin matrix within control and test cell layers. Fluorescence (red) due to LOX expression was also much more intense in cell layers that received CuNPs (400 ng ml^{-1}) alone or together with HA oligomers than in control cell layers. This confirms the outcomes of our biochemical measurements of LOX protein synthesis (Fig. 3B). The matrices also showed presence of fibrillin-1 microfibrils, which confirmed normal mechanisms of elastin fiber assembly. The literature indicates that the fibrillin microfibrils guide the alignment of tropoelastin molecules for crosslinking and fiber formation [43]. This initial alignment is stabilized by copper ion-dependent LOX, which oxidizes the lysine residues of the aligned elastin molecules and enables crosslinking. Thus, these stabilized and aligned elastin structures act as nucleation sites for further coacervation and crosslinking of more tropoelastin, resulting in organized elastic fiber growth. The presence of highly anionic HA oligomers might also promote elastic fiber formation by electrostatically binding to the unoxidized lysine residues of newly synthesized tropoelastin during their association with microfibrils, thus preventing their random self-aggregation far away from the site of fiber formation [42]. However, these are only possibilities which remain to be investigated in future studies.

5. Conclusions

This study demonstrates the utility of CuNPs as effective vehicles for Cu^{2+} ion delivery to in vitro cultures for improved fibrous elastin matrix assembly. Although exogenous CuNP supplements do not upregulate tropoelastin production by vascular SMCs, they are highly effective in promoting crosslinked elastin matrix formation. The additional presence of HA oligomers within these CuNP-stimulated cultures further improves the deposition of crosslinked matrix elastin. Structural analysis of the isolated matrix elastin reveals the presence of aggregating elastin fibrils within SMC cultures treated with CuNPs (1–10 ng ml^{-1}) alone or together with HA oligomers, different from the amorphous elastin clumps observed within non-additive control cultures. The addition of 400 ng ml^{-1} of CuNPs concurrent with HA oligomers further enhances aggregation of these elastin fibrils, into mature fibers with diameters ranging from 200 to 500 nm. Immunofluorescence imaging and ultrastructural analysis of the elastin matrices with 400 ng ml of CuNP-treated cultures suggest elastin matrix deposition as stimulated by Cu^{2+} ions and HA oligomers proceeds normally via a fibrillin-mediated assembly process, with enhanced crosslinking occurring via stimulation of LOX. Overall, the results attest to the combined benefits of CuNPs and HA oligomers to the regeneration of highly crosslinked fibrillar elastin matrices by adult vascular smooth muscle cells cultures, with immense potential applications to tissue engineering elastin-rich tissue constructs, incorporating elastogenically deficient adult patient cells, for clinical use.

Acknowledgements

References

1. Kielty CM, Sherratt MJ, Shuttleworth CA. Elastic fibres. J Cell Sci 2002;115:2817–2828. [PubMed: 12082143]

2. Brooke BS, Bayes-Genis A, Li DY. New insights into elastin and vascular disease. Trends Cardiovasc Med 2003;13:176–181. [PubMed: 12837579]

3. Hinek A, Wrenn DS, Mecham RP, Barondes SH. The elastin receptor: a galactoside-binding protein. Science 1988;239:1539–1541. [PubMed: 2832941]

4. Li DY, Brooke B, Davis EC, Mecham RP, Sorensen LK, Boak BB, Eichwald E, Keating MT. Elastin is an essential determinant of arterial morphogenesis. Nature 1998;393:276–280. [PubMed: 9607766]

5. Kielty CM, Stephan S, Sherratt MJ, Williamson M, Shuttleworth CA. Applying elastic fibre biology in vascular tissue engineering. Phil Trans R Soc B 2007;362:1293–1312. [PubMed: 17588872]

6. Mitchell SL, Niklason LE. Requirements for growing tissue-engineered vascular grafts. Cardiovasc Pathol 2003;12:59–64. [PubMed: 12684159]

7. Bellingham CM, Lillie MA, Gosline JM, Wright GM, Starcher BC, Bailey AJ, Woodhouse KA, Keeley FW. Recombinant human elastin polypeptides self-assemble into biomaterials with elastin-like properties. Biopolymers 2003;70:445–455. [PubMed: 14648756]

8. Mithieux SM, Rasko JE, Weiss AS. Synthetic elastin hydrogels derived from massive elastic assemblies of self-organized human protein monomers. Biomaterials 2004;25:4921–4927. [PubMed: 15109852]

9. Wright ER, Conticello VP. Self-assembly of block copolymers derived from elastin-mimetic polypeptide sequences. Adv Drug Deliv Rev 2002;54:1057–1073. [PubMed: 12384307]

10. Radhakrishnamurthy B, Ruiz H, Berenson GS. Interactions of glycosaminglycans with collagen and elastin in bovine aorta. Adv Exp Med Biol 1977;82:160–163. [PubMed: 920351]

11. Bartholomew JS, Anderson JC. Investigation of relationships between collagens, elastin and proteoglycans in bovine thoracic aorta by immunofluorescence techniques. Histochem J 1983;15:1177–1190. [PubMed: 6358143]

12. Joddar B, Ramamurthi A. Fragment size- and dose-specific effects of hyaluronan on matrix synthesis by vascular smooth muscle cells. Biomaterials 2006;27:2994–3004. [PubMed: 16457881]

13. Joddar B, Ramamurthi A. Elastogenic effects of exogenous hyaluronan oligosaccharides on vascular smooth muscle cells. Biomaterials 2006;27:5698–5707. [PubMed: 16899292]

14. Kothapalli CR, Ramamurthi A. Benefits of concurrent delivery of hyaluronan and IGF-1 cues to regeneration of crosslinked elastin matrices by adult rat vascular cells. J Tissue Eng Regen Med 2008;2:106–116. [PubMed: 18338830]

15. Kothapalli CR, Taylor PM, Smolenski RT, Yacoub MH, Ramamurthi A. TGF-β1 and hyaluronan oligomers synergistically enhance elastin matrix regeneration by vascular smooth muscle Cells. Tissue Eng. 2008In Press

16. Gacheru S, Trackman PC, Shah MA, O'Gara CY, Spacciapoli P, Greenaway FT, Kagan HM. Structural and catalytic properties of copper in lysyl oxidase. J Biol Chem 1990;265:19022–19027. [PubMed: 1977746]

17. Kagan HM, Li W. Lysyl oxidase: properties, specificity, and biological roles inside and outside of the cell. J Cell Biochem 2003;88:660–672. [PubMed: 12577300]

18. Rucker R, Kosonen T, Clegg MS, Mitchell AE, Rucker RB, Uriu-Hare JY, Keen CL. Copper, lysyl oxidase, and extracellular matrix protein crosslinking. Am J Clin Nutr 1998;67:996S–1000S. [PubMed: 9587142]

19. Kishimoto T, Fukuzawa Y, Abe M, Hashimoto M, Ohno M, Tada M. Injury to cultured human vascular endothelial cells by copper (CuSO4). Nippon Eiseigaku Zasshi 1992;47:965–970. [PubMed: 1287265]

20. Rowley D, Halliwell B. Superoxide-dependent and ascorbate-dependent formation of hydroxyl radicals in the presence of copper salts: A physiologically significant reaction? Arch Biochem Biophys 1983;225:279–284. [PubMed: 6311105]

21. Cortizo MC, Fernandez Lorenzo de Mele M. Cytotoxicity of copper ions released from metal: variation with the exposure period and concentration gradients. Biol Trace Elem Res 2004;102:129–141. [PubMed: 15621934]

22. Kothapalli CR, Ramamurthi A. Biomimetic regeneration of elastin matrix structures using hyaluronan and copper ion cues. Tissue Eng. 2008In Press

23. Labarca C, Paigen K. A simple, rapid, and sensitive DNA assay. Anal Biochem 1980;102:344–352. [PubMed: 6158890]

24. Liao J, Vesely I. Relationship between collagen fibrils, glycosaminoglycans, and stress relaxation in mitral valve chordae tendineae. Ann Biomed Eng 2004;32:977–983. [PubMed: 15298435]

25. Trackman PC, Zoski CG, Kagan HM. Development of a peroxidase-coupled fluorometric assay for lysyl oxidase. Anal Biochem 1981;113(2):336–42. [PubMed: 6116464]

26. Jaakkola K, Kaunismäki K, Tohka S, Yegutkin G, Vänttinen E, Havia T, Pelliniemi LJ, Virolainen M, Jalkanen S, Salmi M. Human vascular adhesion protein-1 in smooth muscle cells. Am J Pathol 1999;155(6):1953–65. [PubMed: 10595925]

27. Ashworth JL, Murphy G, Rock MJ, Sherratt MJ, Shapiro SD, Shuttleworth CA. Fibrillin degradation by matrix metalloproteinases: implications for connective tissue remodelling. Biochem J 1999;340:171–181. [PubMed: 10229672]

28. Shapiro SD. Matrix metalloproteinase degradation of extracellular matrix: biological consequences. Curr Opin Cell Biol 1998;10:602–608. [PubMed: 9818170]

29. Jacob MP. Extracellular matrix remodeling and matrix metalloproteinases in the vascular wall during ageing and in pathological conditions. Biomed Pharmacol 2003;57:195–200.

30. D'Armiento J. Decreased elastin in vessel walls puts the pressure on. J Clin Invest 2003;112:1308–1310. [PubMed: 14597755]

31. Safar ME, Levy BI, Struijker-Boudier H. Current perspectives on arterial stiffness and pulse pressure in hypertension and cardiovascular diseases. Circulation 2003;107:2864–2869. [PubMed: 12796414]

32. Franzblau C. Elastin. Comprehensive Biochem 1971;26c:659–712.

33. Mecham, RP.; Davis, EC. Elastic fiber structure and assembly. In: Yurchenco, PD.; Birk, DE.; Mecham, RP., editors. Extracellular Matrix Assembly And Structure. New York: Academic Press; 1994. p. 281-314.

34. Csiszar K. Lysyl oxidases: a novel multifunctional amine oxidase family. Prog Nucleic Acid Res Mol Biol 2001;70:1–32. [PubMed: 11642359]

35. Cleary EG, Gibson MA. Elastin-associated microfibrils and microfibrillar proteins. Int Rev Connect Tissue Res 1983;10:97–209. [PubMed: 6358100]

36. Johnson DJ, Robson P, Hew Y, Keeley FW. Decreased elastin synthesis in normal development and in long-term aortic organ and cell cultures is related to rapid and selective destabilization of mRNA for elastin. Circ Res 1995;77:1107–1113. [PubMed: 7586222]

37. McMahon MP, Faris B, Wolfe BL, Brown KE, Pratt CA, Toselli P, Franzblau C. Aging effects on the elastin composition in the extracellular matrix of cultured rat aortic smooth muscle cells. In Vitro Cell Dev Biol 1985;21:674–680. [PubMed: 3908442]

38. Opitz F, Schenke-Layland K, Cohnert TU, Starcher B, Halbhuber KJ, Martin DP, Stock UA. Tissue engineering of aortic tissue: dire consequence of suboptimal elastic fiber synthesis in vivo. Cardiovasc Res 2004;63:719–730. [PubMed: 15306228]

39. Ramamurthi A, Vesely I. Evaluation of the matrix-synthesis potential of crosslinked hyaluronan gels for tissue engineering of aortic heart valves. Biomaterials 2005;26:999–1010. [PubMed: 15369688]

40. Dahl SLM, Rucker RB, Niklason LE. Effects of copper and cross-linking on the extracelluar matrix if tissue-engineered arteries. Cell Transplantation 2005;14:367–374. [PubMed: 16180655]

41. Barbucci R, Lamponi S, Magnani A, Piras FM, Rossi A, Weber E. Role of the Hyal-Cu (II) complex on bovine aortic and lymphatic endothelial cells behavior on microstructured surfaces. Biomacromolecules 2005;6:212–9. [PubMed: 15638523]

42. Fornieri C, Baccarani-Contri M, Quaglino D Jr, Pasquali-Ronchetti I. Lysyl oxidase activity and elastin/glycosaminoglycan interactions in growing chick and rat aortas. J Cell Biol 1987;105:1463–1469. [PubMed: 2888772]

43. Augsburger PB, Tisdale C, Broekelmann T, Sloan C, Mecham RP. Identification of an elastin cross-linking domain that joins three peptide chains. J Biol Chem 1995;270:17778. [PubMed: 7629078]
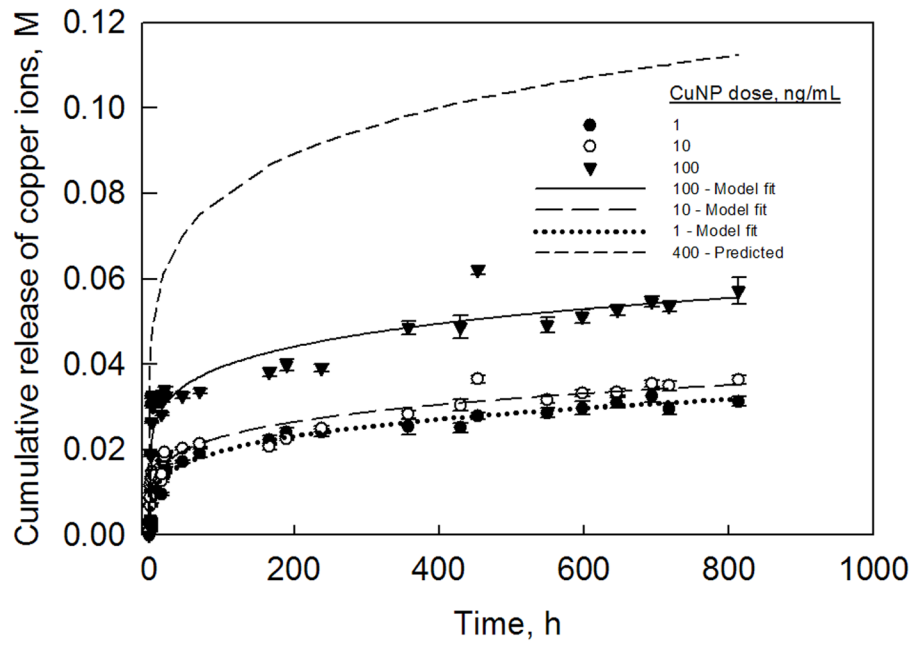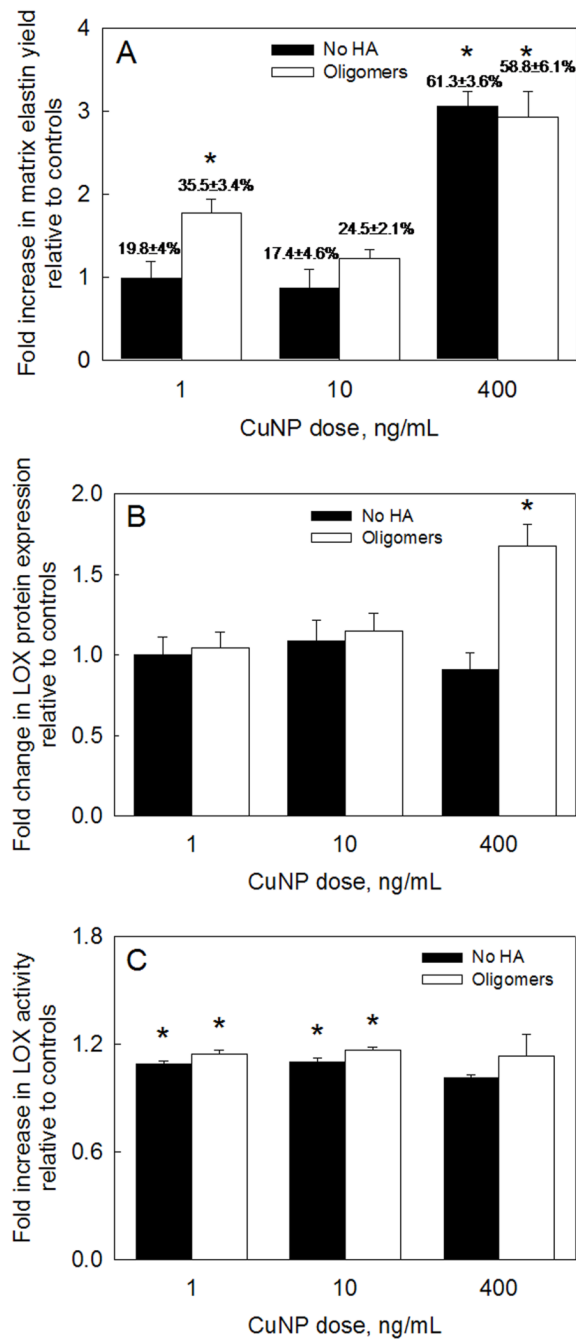
Figure 1.
Copper ion release profiles from CuNPs (1–100 ng ml^{-1}) in distilled water. The profiles were fitted with hierarchical regression analysis model described by Eq. (1). Based on this model, the CuNP dose that cumulatively releases ~0.1 M of Cu^{2+} ions over a 21 day period was determined to be 400 ng ml^{-1}.
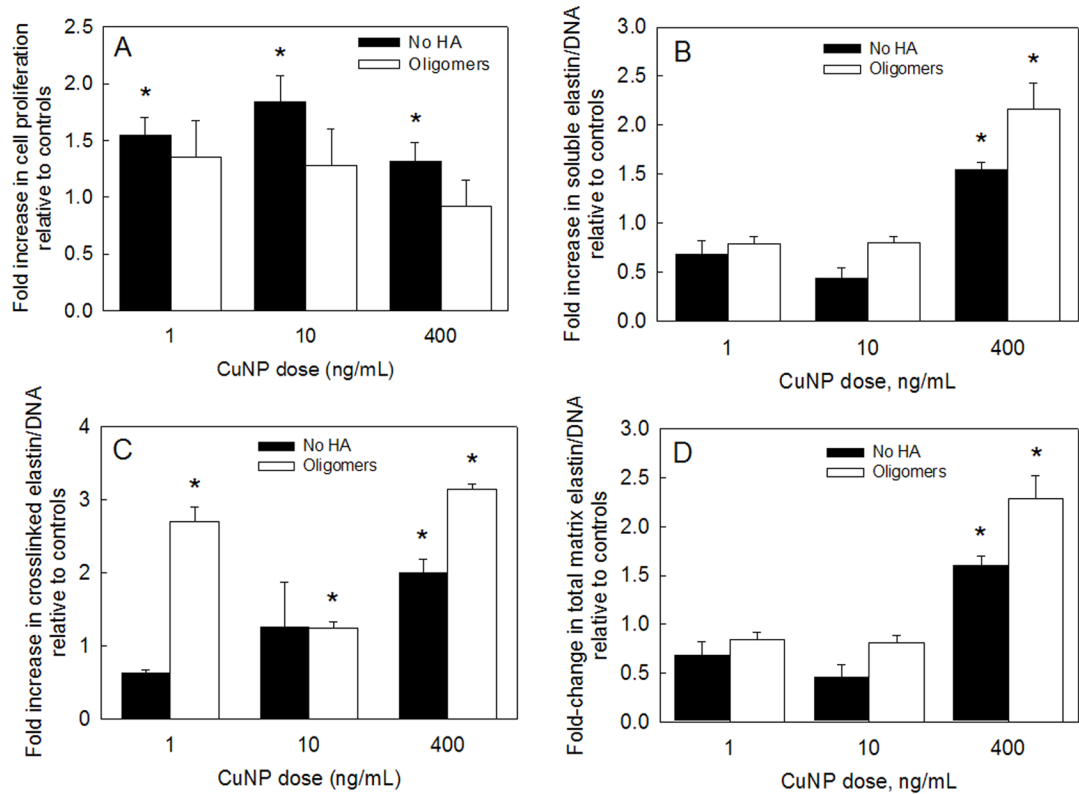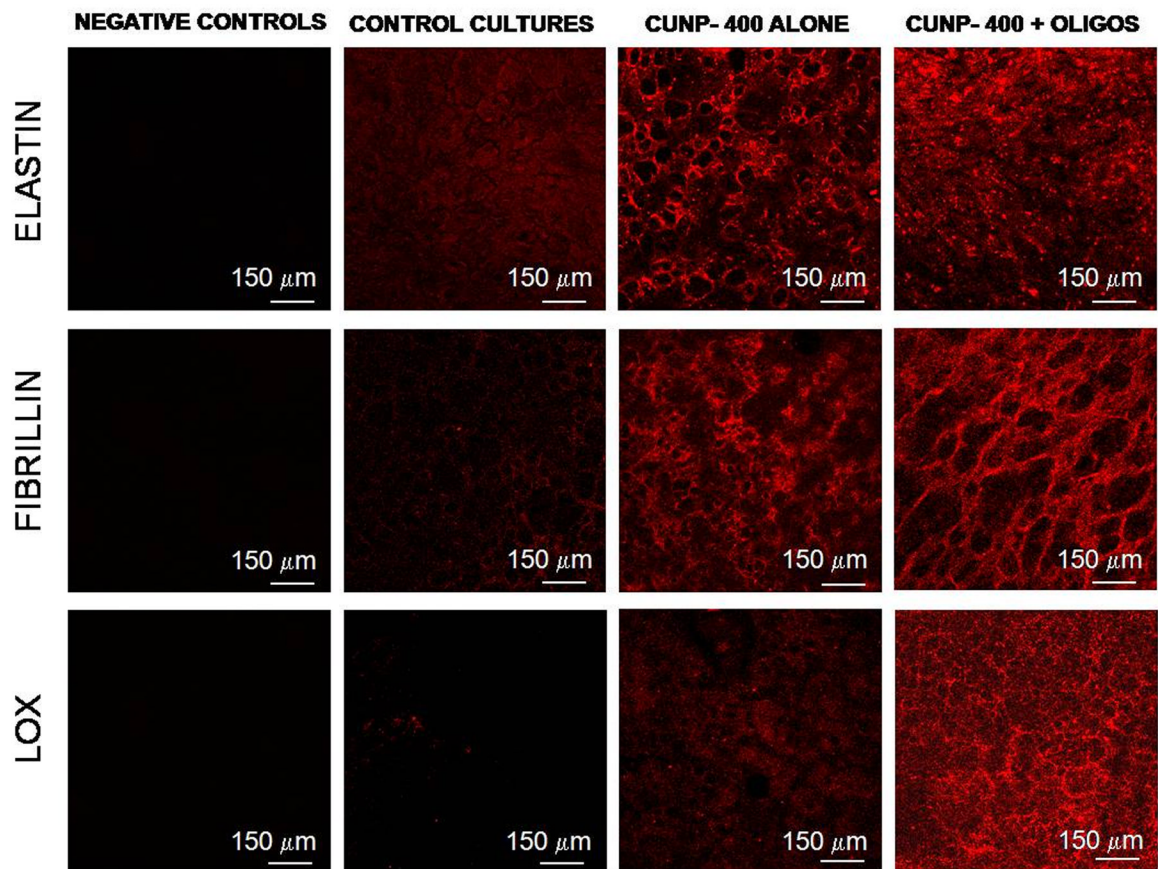
Figure 2.
(A) Proliferation ratios of RASMCs supplemented with CuNPs (1–400 ng ml^{-1}) alone or together with HA oligomers (0.2 μg ml^{-1}). Data shown represent mean ± SD of cell count after 21 days of culture, normalized to initial seeding density and further normalized to control cultures that received no additives (n = 3 per case). Effects of exogenous CuNPs with or without HA oligomers on alkali-soluble matrix elastin (B), crosslinked alkali-insoluble matrix elastin (C) and total matrix elastin (D), synthesized by adult RASMCs. Values (mean ± SD) are shown normalized to the DNA content of the respective cell layers at 21 days of culture (n = 3 per case) relative to control cultures. * represents significant differences relative to control cultures ($P < 0.05$).
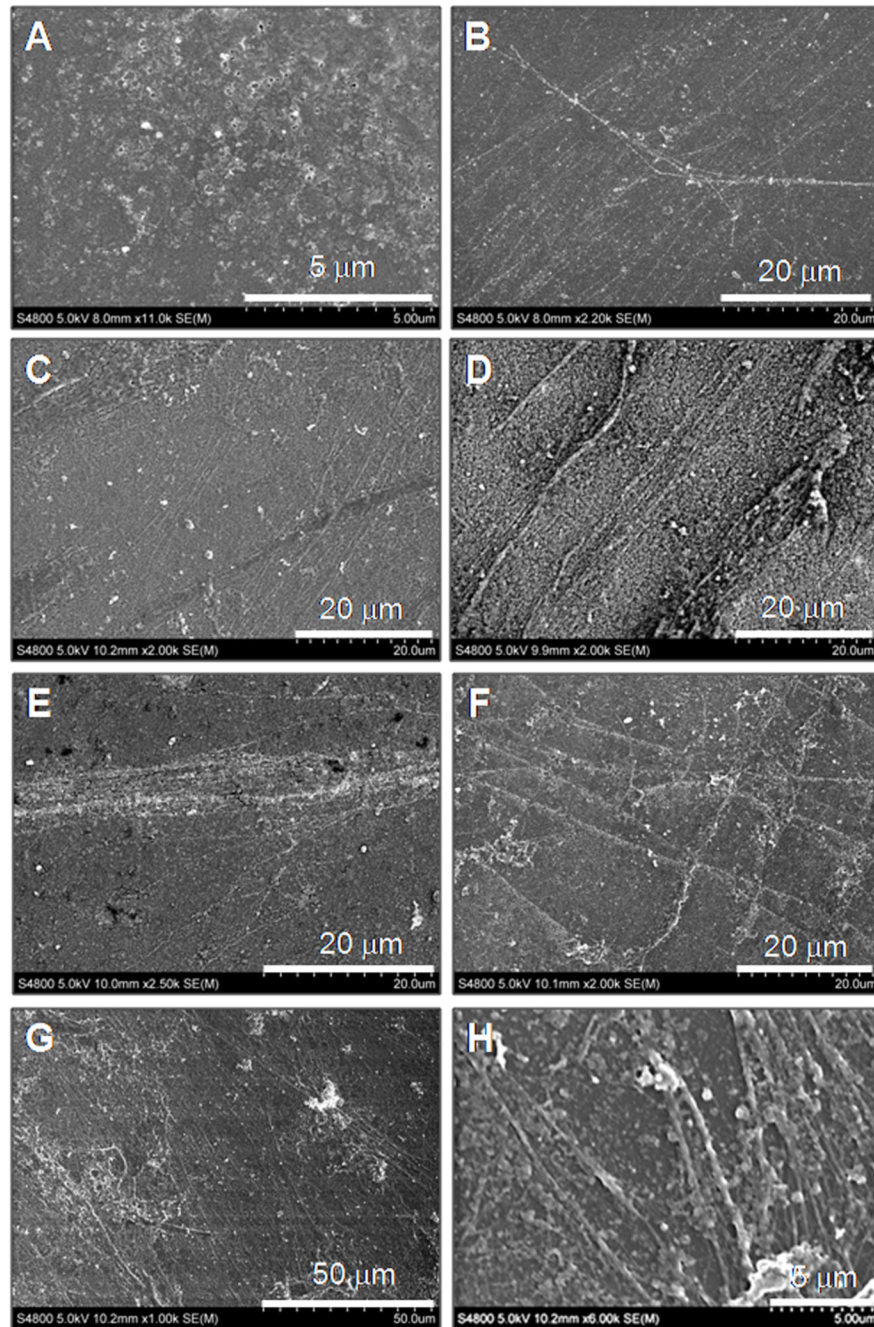
Figure 3.
(A) Matrix elastin yield within RASMC cultures supplemented with CuNPs and HA oligomers. The ratio of matrix elastin deposited to total elastin synthesized was calculated in each test case and was further normalized to similar ratio in control cultures. (B) LOX protein amounts in pooled medium aliquots collected over 21 days of culture. Shown are mean ± SD of DNA-normalized intensities, measured from representative SDS-PAGE/Western blots containing bands corresponding to LOX produced in the respective cases. (C) LOX enzyme activities in cultures treated with CuNPs and HA oligomers. Values (mean ± SD) are shown normalized to the LOX activity measured in control cell layers at 21 days of culture (n = 3 per case). * represents significance in differences relative to controls ($P < 0.05$).
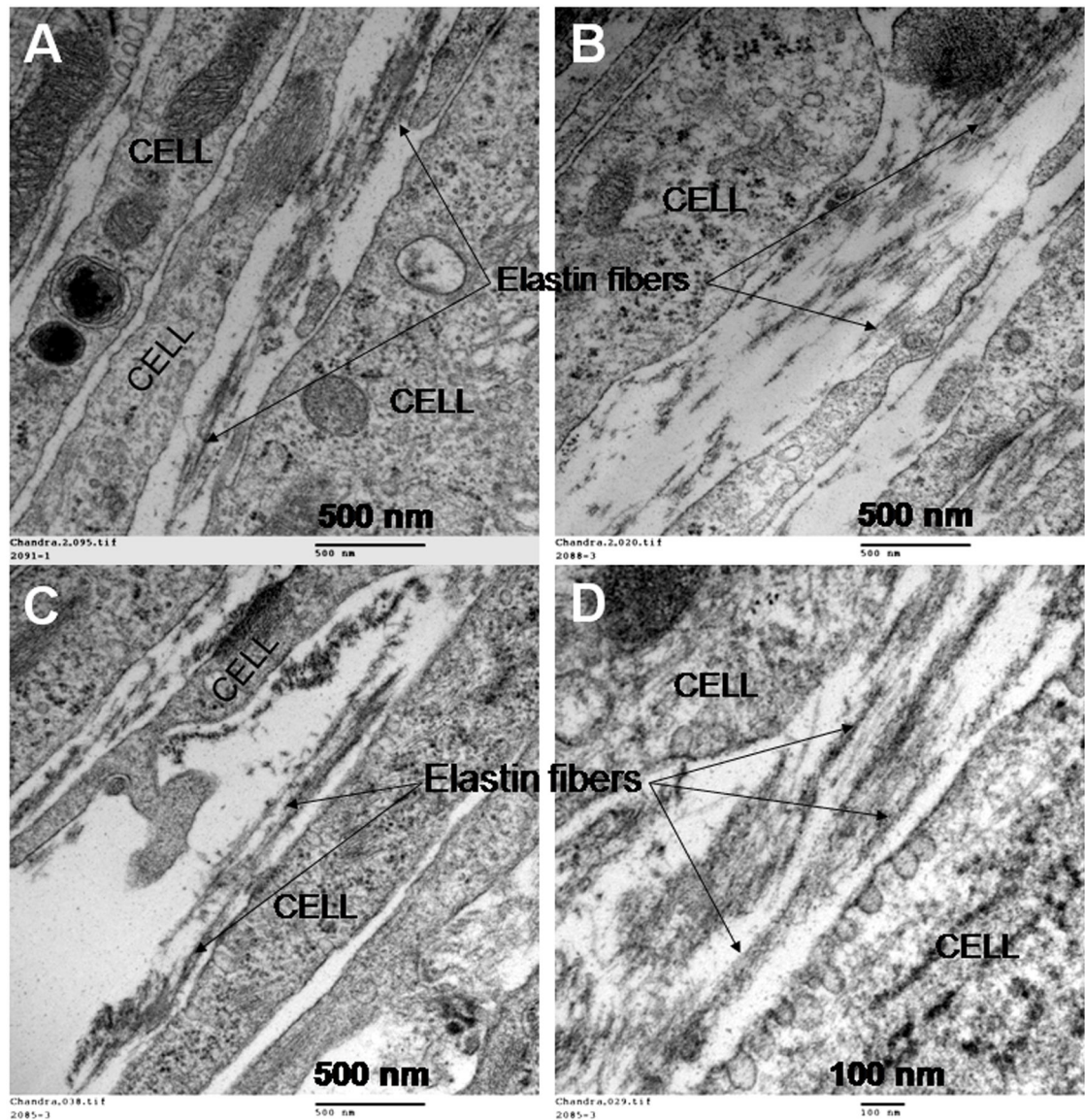
Figure 4.
Immunodetection of elastin, fibrillin and LOX (red) within RASMC layers following 21 days of culture in the presence of 400 ng ml^{-1} of CuNPs alone or together with HA oligomers (0.2 µg ml^{-1}); control cultures received no additives. Immunolabeling controls received no primary antibodies and exhibited no background fluorescence when treated with the fluorophore-labeled secondary probe.

Figure 5.
Representative SEM images of 21 day old RASMC cell layers for non-additive controls (panel A); cultured with CuNPs alone (1 ng ml^{-1}: panel B; 10 ng ml^{-1}: panel C; 400 ng ml^{-1}: panel D); cultured with CuNPs and HA oligomers (1 ng ml^{-1}: panel E; 10 ng ml^{-1}: panel F; 400 ng ml^{-1}: panels G, H). Compared to CuNP-supplemented cultures, the additional presence of oligomers enhanced the formation of dense crosslinked matrix elastin fibers with diameters ranging between 0.2 and 0.5 μm.

Figure 6.
Representative TEM images of 21 day old RASMC cell layers cultured additive-free (A), with CuNPs alone (400 ng/ml^{-1}; panel B) or together with HA oligomers (panels C and D). Aggregating amorphous elastin clumps leading to the formation of elastin fibers can be clearly seen in these images (panel C), which confirm the identity of elastin observed at higher magnifications (100000×; panel D).